Changes in short-range order in the alloy $Fe_{83}Si_{17}$ due to heat treatment and plastic deformation

1989 J. Phys.: Condens. Matter 1 4749

(http://iopscience.iop.org/0953-8984/1/29/001)

J. Phys.: Condens. Matter **1** (1989) 4749–4754. Printed in the UK

Changes in short-range order in the alloy $Fe_{83}Si_{17}$ due to heat treatment and plastic deformation

O Schneeweiss
Institute of Physical Metallurgy, Czechoslovak Academy of Sciences, Žižkova 22, CS-616 62 Brno, Czechoslovakia

Received 3 June 1988, in final form 24 November 1988

Abstract. The structures of samples of the alloy $Fe_{83}Si_{17}$ after different methods of heat treatment and a high degree of plastic deformation were investigated from the point of view of their short-range order (SRO). The SRO of the annealed and slowly cooled sample was compared with that of the samples prepared by methods of rapid quenching from the melt (double roller quenching, spark erosion and laser surface treatment) and with the powder prepared by mechanical crushing. The more important differences were observed in the spark-eroded powder and in the crushed powder where amorphisation of the structure occurs. The cause of the transformation to the amorphous state is the high density of defects introduced in the sample. A quenching rate of the melt of up to 10^6 K s^{-1} does not seem to be rapid enough to cause a change in the SRO of this alloy.

1. Introduction

It has been shown in several papers reporting studies of the structure of Fe–Si alloys with more than 12 at.% Si that the structure characterised by long-range order (LRO) and also short-range order (SRO) is very stable relative to the heat treatment (Glaser and Ivanick 1956, Meinhardt and Krisement 1965, Gemperle 1968, Häggström *et al* 1973). Mangin *et al* (1976) and Yamakawa and Fujita (1979) have observed an amorphous state in thin films prepared by vapour deposition. Yelsukov *et al* (1983) have observed important changes in the structure due to plastic deformation. According to the phase diagram of Fe–Si binary alloys (Massalski 1986) the alloy $Fe_{83}Si_{17}$ should yield samples with different types of LRO. After rapid quenching from 1200 °C, it should be possible to fix the α-phase (disordered solid solution) and similarly the α_2-phase (superstructure B2) should appear after quenching from 1050 °C. Annealing at temperatures below 960 °C should yield samples with the α_1-phase (superstructure DO_3). However, the investigation of the structure of the samples annealed at 1200 and 1050 °C and quenched in the cooling liquid did not show any difference from the α_1-phase (Schneeweiss 1979).

The aim of this work is to study the SRO in the alloy $Fe_{83}Si_{17}$ after quenching from the liquid state at different quenching rates and after plastic deformation. Mössbauer spectroscopy was used for this purpose and gives information about the SRO in ferromagnetic iron alloys (Fujita 1975).

0953-8984/89/294749 + 06 $02.50

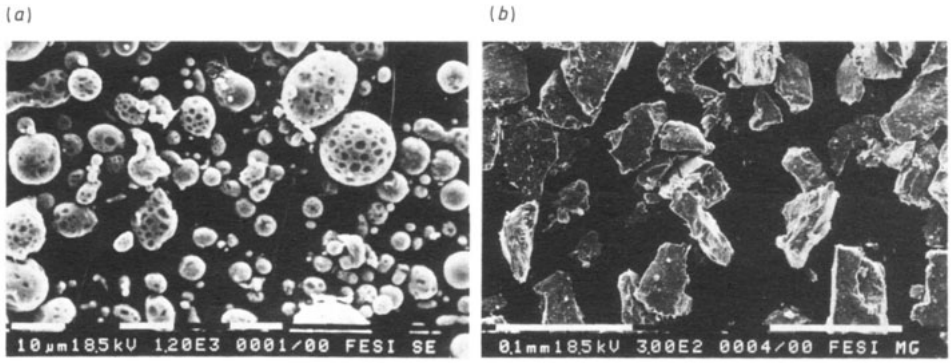

Figure 1. SEM micrographs of (*a*) the spark-eroded and (*b*) the mechanically crushed powders

2. Experimental details

The alloy $Fe_{83}Si_{17}$ was prepared from pure (99.9%) iron and pure (99.99%) silicon by melting in an alumina crucible. From this alloy the following samples were prepared:

(i) foil 40 μm thick made by surface grinding and chemical etching from the ingot subsequently annealed at 800 °C for 1 h in vacuum and slowly cooled in the furnace;

(ii) ribbon about 30 μm thick made by the double-roller quenching technique using rapidly rotating steel rollers;

(iii) particles 1–20 μm in diameter (figure 1(*a*)) obtained by spark erosion of the ingot;

(iv) sheet 2 mm thick with a surface laser treated in argon;

(v) powder made by mechanical crushing in an agate mortar and passed through sieves (figure 1(*b*)).

The laser surface treatment was performed under two conditions: neodymium laser 4 μs pulses of 0.5 J and 4 J with 0.3 mm and 1 mm spot diameters, respectively. Optical metallography showed that the remelted area is roughly 100 μm deep. It is very difficult to obtain a high degree of plastic deformation by means of standard methods, e.g. tensile stress or rolling, because of the high hardness and poor ductility of this alloy at room temperature. This is why a crushed powder has been investigated as a sample having a high degree of plastic deformation. A rough but simple estimation of the degree of plastic deformation was made by measuring the mean size of the powder particles (Arita *et al* 1985). The chemical composition of samples as checked by means of energy-dispersive micro-analysis agreed with the nominal composition of the alloy and no increase in the impurity contents was found.

Mössbauer spectra were recorded at room temperature using a ^{57}Co in chromium source. The thin foils and powder samples were measured in transmission geometry with γ-ray detection. The spectra of the thick sheets and the surface of the powders were measured in scattering geometry detecting conversion electrons. All velocities are given relative to α-iron. Spectrum analysis was performed by least-squares fits to sets of Lorentzian lines.

3. Results

In interpreting the results from the point of view of SRO the procedure published formerly was applied (Schneeweiss 1986). Some examples of the spectra and the fitted curves are

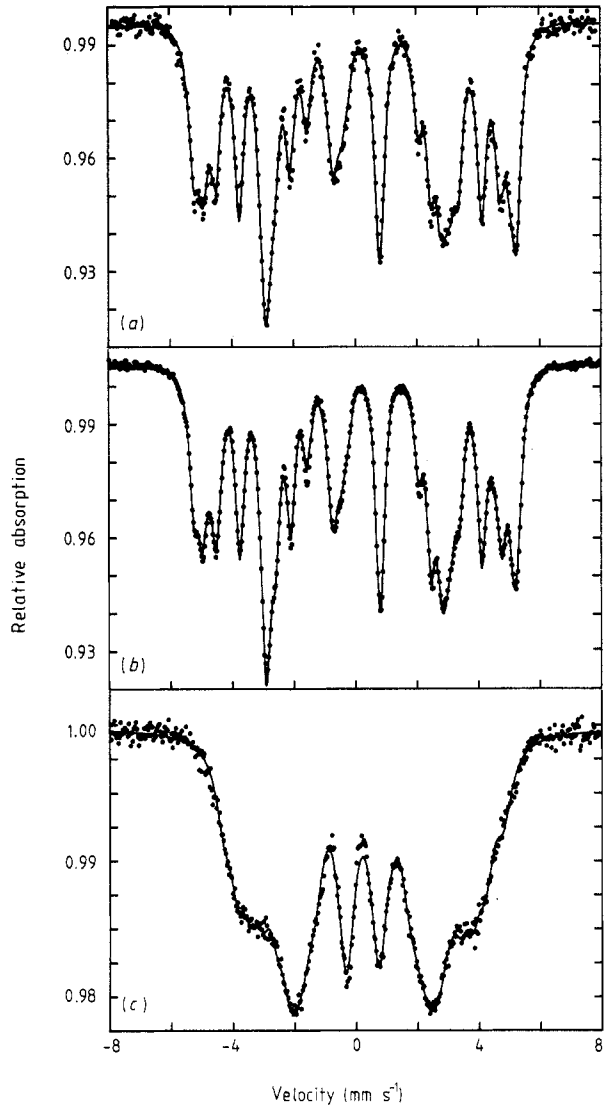

Figure 2. Mössbauer spectra: (*a*) sample (i); (*b*) sample (ii); (*c*) sample (iii).

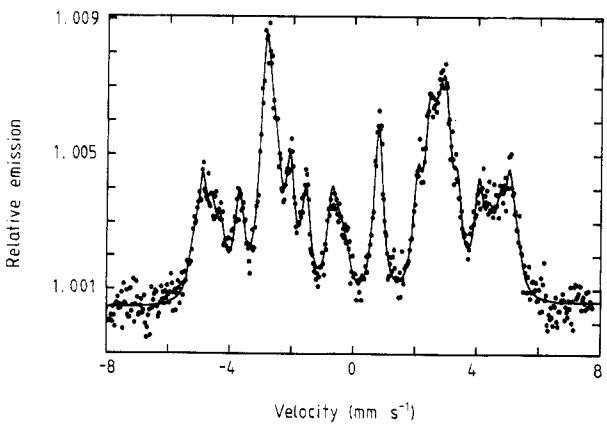

Figure 3. Mössbauer spectrum of sample (iv). The parameters of the laser pulses were 4 μs, 0.5 J and 0.3 mm.

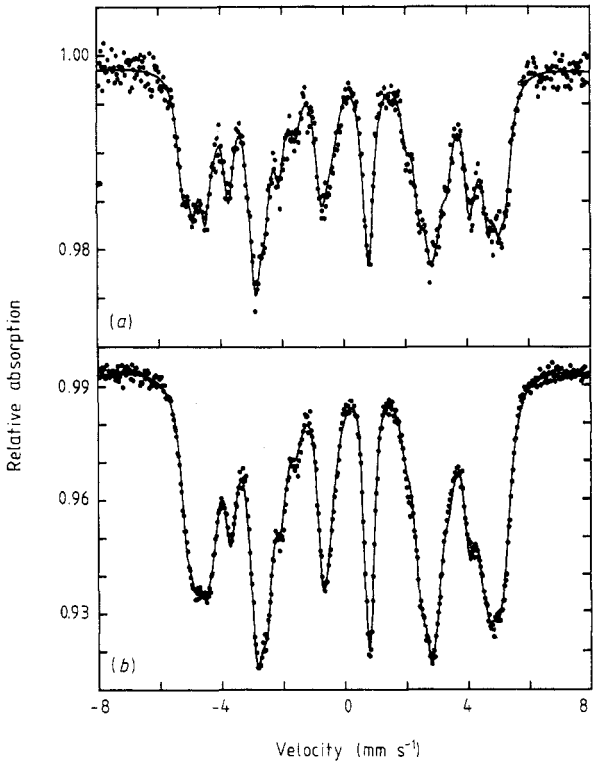

Figure 4. Mössbauer spectra of samples (v) for mean particle diameters (*a*) 54 μm and (*b*) 29 μm.

Table 1. Comparison of the experimental intensities of the most important iron surroundings with the values derived from the model of a random distribution of single silicon atoms and the model of pairs of silicon atoms. $P(k, l)$ is the intensity of iron atoms with k and l silicon atoms as nearest and second-nearest neighbours, respectively.

$P(k, l)$	Experimental	Random distribution	Silicon pairs
$\Sigma_l(0, l)$	0.378 ± 0.017	0.402	0.398
(2, 0)	0.146 ± 0.010	0.167	0.142
(3, 0)	0.248 ± 0.006	0.245	0.249
(4, 0)	0.175 ± 0.006	0.135	0.167
(5, 0)	—	0.000	0.000

shown in figures 2–4. The model of SRO giving the best fit of the sample (i) spectrum is compatible with the DO_3 superstructure, where the silicon atoms prefer clusters in the form of pairs of silicon atoms. The distance between the silicon atoms is equal to the length of the face diagonal of the BCC unit cell. This is demonstrated in table 1 where the experimental data derived from the spectrum of sample (i) are compared with the model assuming a random distribution of single silicon atoms and with the model based on the pairs of silicon atoms. Both models are compatible with DO_3 superstructure. The same model of SRO can be applied to sample (ii). The spectrum of sample (iii) differs substantially from the spectra of both previous samples. Its shape and parameters are similar to the spectra of the amorphous samples of Mangin *et al* (1976). To exclude the influence

of the particle size or superparamagnetic behaviour on the spectrum shape the same sample was measured after additional annealing at 800 °C for 1 h in vacuum. The SRO in the sample after this treatment agrees with that in sample (i), which means that the particle size does not play an important role. The SRO of the surface layer of sample (iv) is also very similar to that of sample (i) and is not dependent on the condition of laser irradiation, e.g. the energy density of the photon beam. The analysis of the influence of plastic deformation on the SRO shows coexistence of the SRO of the annealed bulk material and an amorphous phase. In the spectra shown in figure 4 the part corresponding to the amorphous phase occupies 6% and 17% for the powders having mean particle diameters of 54 μm and 29 μm, respectively. The amorphous phase content increases with increasing degree of deformation. Also, in this case, annealing at 800 °C for 1 h in vacuum makes the SRO change to the same state as in sample (i). No differences were found between the spectra of whole powder particles and those of their surface. This means that the process of amorphization due to plastic deformation occurs in the whole powder particles.

4. Discussion

In the investigated samples, two different phases were observed. One is the crystalline α_1-phase characterised by SRO compatible with the $D0_3$ superstructure and by preference of silicon atom pairs as third-nearest neighbours. The other is an amorphous phase. The crystalline α_1-phase is even formed in the ribbons prepared from the melt at a quenching rate of about 10^5 K s^{-1}. The amorphous structure was observed in spark-eroded particles where the quenching rate reaches 10^6 K s^{-1} (Berkowitz and Walter 1987). The higher quenching rate (10^8 K s^{-1} according to Heinemann (1985)) enables laser irradiation to be used. From this point of view the SRO found on the surface after laser irradiation is surprising, but a simple explanation of this discrepancy can be given if the integral process of irradiation is taken into account. Data on the quenching rate are given for a single pulse of photons. After irradiation of a large area, all spots (excluding the last one) are surrounded by spots irradiated later. The heat produced by the later pulses causes annealing of previous spots and this could be sufficient to bring about transformation from the amorphous to the α_1-phase. This is also indirect proof of the growth rate of the SRO detected in the double-roller-quenched ribbon.

Amorphisation due to a high degree of plastic deformation in the crushed powder originates from regions with a high density of defects which are transformed spontaneously to the amorphous state owing to a free-energy minimum (Frenkel 1958, Vepřek *et al* 1982, Pavlov 1985). The coexistence of both crystalline and amorphous phases in the powder sample might be explained because the critical density of defects in powder particles is not reached simultaneously but successively. A similar explanation of the amorphous state can be given for spark-eroded particles. Fine droplets of the liquid alloy produced during spark discharges are spread from the electrode in a dielectric liquid (e.g. kerosene) and rapidly quenched. Solidification begins on the whole surface of the droplets. Thus this creates on the droplet surface a large number of solid state embryos which are oriented randomly, and therefore a high density of non-coherent boundaries must be formed. The density of defects exceeds the critical value and the amorphous state is more advantageous. It should be mentioned that the surface-to-volume ratio of the quenched material is 10 times higher in the spark erosion process than

in double-roller quenching. Besides the quenching rate this is an additional difference between the two methods.

The results mentioned above show the high rate of formation of the SRO of $D0_3$ type in the alloy $Fe_{83}Si_{17}$ and confirm its high stability. No other type of SRO, e.g. one compatible with the B2 superstructure or with the solid solution, was observed. Instead of a change in the SRO, a transformation to the amorphous state occurs when a high density of defects is introduced into the sample.

References

Arita M, Nasu S and Fujita F E 1985 *Trans. Japan Inst. Metall.* **26** 710

Berkowitz A E and Walter J L 1987 *J. Mater. Res.* **2** 277

Frenkel Ya I 1958 *Introduction to the Theory of Metals* (Moscow: Fizmatgiz) p 220

Fujita F E 1975 *Springer Topics in Applied Physics* vol 5, ed. U Gonser (Berlin: Springer) p 224

Gemperle A 1968 *Trans. AIME* **242** 2287

Glaser F W and Ivanick W 1956 *J. Met.* **8** 1290

Häggström L, Granäs L, Wäppling R and Devanarayanan S 1973 *Phys. Scr.* **7** 125

Heinemann W A 1985 *Proc. 5th Conf. Rapidly Quenched Metals Würzburg, 1984* ed. S Steeb and H Warlimont (Amsterdam: North-Holland) p 27

Mangin P, Marchal G, Piecuch M and Janot C 1976 *J. Phys. E: Sci. Instrum.* **9** 1101

Massalski T B (ed.) 1986 *Binary Alloy Phase Diagrams* (Metals Park, OH: American Society for Metals) p 1108

Meinhardt R N and Krisement O 1965 *Arch. Eisenhüttenwes.* **36** 193

Pavlov V A 1985 *Fiz. Metall. Metalloved.* **59** 629

Schneeweiss O 1979 *PhD Thesis* Institute of Physical Metallurgy, Brno

—— 1986 *J. Magn. Magn. Mater.* **58** 163

Vepřek S, Iqbal Z and Sarott F-A 1982 *Phil. Mag.* B **45** 137

Yamakawa Y and Fujita F E 1979 *J. Physique Coll.* **40** C2 101

Yelsukov Ye P, Barinov V A, Galakhov V R, Yurchikov Ye Ye and Yermakov A Ye 1983 *Fiz. Metall. Metalloved.* **55** 337